

Rheological properties of melt-compounded and diluted nanocomposites of atomic-layer-deposition-coated polyamide particles

Katja Nevalainen¹, Christian Hintze², Reija Suihkonen¹, Pirkko Eteläaho¹,
Jyrki Vuorinen¹, Pentti Järvelä¹, Nora Isomäki³

¹ Tampere University of Technology / Laboratory of Plastics and Elastomer Technology, Tampere, Finland
² Chemnitz University of Technology / Faculty of Mechanical Engineering, Chemnitz, Germany
³ Beneq Oy, Espoo, Finland

ABSTRACT

Polyamide particles were coated successfully with titanium dioxide films by atomic-layer-deposition and subsequent melt-compounding to form polyamide nanocomposites. The rheological properties of these materials, characterized by melt flow indexer, melt flow spiral mould, and rotational rheometer, demonstrated significantly lower viscosity for the nanocomposites than for pure polyamide.

INTRODUCTION

The potential of atomic layer deposition (ALD) in nanotechnology has been recognized for years^{1,2}. ALD is a versatile tool for nanotechnology because it enables the growth of nanometer-scale films on virtually any size or shape substrates. It is a method based on self-limiting chemical reactions of molecular species from the gas phase due to parameters such as precursor and purge gas pulse times as well as reaction temperature. As a result, ALD yields thin films of high-quality materials with excellent film conformality, large surface area capability, good film reproducibility, and easy thickness control. In fact, the feasibility of ALD has been proved with many nanomaterials, nanoparticles, nanolaminates, porous substrates, nanofibers, and nanorods¹⁻³.

Recently, ALD has been applied to producing high-quality polymeric

nanocomposites, but only little data has been published⁴⁻⁶. Spencer et al.⁴, for example, have successfully created polymeric nanocomposites from melt-compounded high-density polyethylene particles coated with nanoscale alumina. A more detailed study on the advantages of ALD technology for polymer nanocomposites was introduced in our previous work⁶ on a titanium-dioxide-thin-film-coated and melt-extruded polyamide matrix. We demonstrated that, in addition to good dispersion, the ALD-created nanocomposite possessed significantly lower melt-processing viscosities than a pure polyamide matrix without deteriorating thermal properties⁶. This unique property combination offers great opportunities, for example, for the injection moulding of micro-products, because it permits easier filling of the mould and thus rapid solidification, yielding high-quality products. Good examples of such precision products in which ALD technology may be advantageous include medical diagnostics and storage devices such as CD-ROMs and DVDs^{7,8}.

A critical issue in the application of ALD technology for the nanocomposite manufacture is, however, the cost. ALD is considered a slow, expensive method with complicated deposition instrumentation and, therefore, unsuitable for high volume manufacture of commercial products^{1,9}. To help ALD-assisted polymer nanocomposite formation become mainstream, a scalable,

cost-effective ALD reactor solution must be developed. Intensive work with good results has been done, for example, on compensating the modest thin film growth rate in the ALD process for more efficient and scalable fluidized bed reactors⁹. Another fascinating solution is the development of the current batch type process into a continuous substrate coating process. However, such developments are extremely time-consuming and expensive. Therefore, as a first step to a more cost-effective commercialization of ALD-created polymeric nanocomposites, we are introducing the application of ALD-coated polymer particles as additives in a polymer matrix, a solution that is very attractive because of its readily verifiable functionality.

The objective of this study was to use titanium dioxide ALD-coated polyamide particles as additives and dilute them with pure polyamide to form polymer nanocomposites. The target was to examine the melt flow behaviour, complex viscosity, and thermal property changes of the ALD-created nanocomposites as a function of dilution proportion and thus understand better the reasons for the marked drop in viscosity in the ALD coating observed in our previous work⁶.

EXPERIMENTAL

Materials used

The polymeric powder used was polyamide PA 2200 (EOS GmbH) with an average particle size of 60 μm ¹⁰. Nanometer-scale thin films of titanium dioxide (TiO_2) were laid on polyamide (PA) particles in a commercial ALD reactor, manufactured by Beneq Oy. The TiO_2 films deposited on PA particles had an approximate nominal thickness of 10 nm or 40 nm. The ALD coating process is described elsewhere⁶.

Melt processing

The ALD-coated PA particles were melt-compounded as received from the ALD reactor. Furthermore, 75%, 50%, and 25%

dilutions of 10-nm-coated PA particles were manufactured (Table 2). The nanocomposites were melt-compounded in a 5-cm³ DSM microextruder, operating at 220°C and 200 rpm with 2-minute dwell time. Subsequent injection moulding of the test specimens (tensile bars and spiral samples) was done using a 5-cm³ DSM injection moulding machine, operating at an injection pressure of about 500 bar, a barrel temperature of 220°C, and a mould temperature of 80°C. In addition, for rheological characterization, disc-like samples with thickness ranging from 80 to 200 μm were prepared using a hot press machine at 200°C and then punched to the desired 25-mm diameter. Prior to each processing step, the raw materials were oven-dried at 80°C for several hours.

Sample characterization

The ALD-coated polyamide powder was examined with a scanning electron microscope (SEM), using Zeiss UltraPlus apparatus equipped with a backscatter electron detector and an energy filter to enable energy selective backscatter (ESB) imaging. Prior to the SEM studies, the powder was cast into an epoxy matrix, and the cured epoxy / ALD-coated powder composite was ground with sand paper to get a cross-sectional figure of the powder particle. The inspected surface was polished with aluminium dioxide. The SEM was operated at an accelerating voltage (electron high tension, EHT) of 15 kV.

The melt-mass flow rate (MFR) of the studied polyamide powders was measured according to SFS ISO 1133 on a CEAST melt flow indexer, model 6452/000, at 191°C under a static load of 2.16 kg.

A melt flow spiral test was run by injecting the polyamide composites into a spiral mould. The material flow distance was then measured to estimate the material's ability to fill a thin-walled part. The flow length was determined as an average of the measured flow lengths of six moulded samples of each material studied. The mould used (Figure 1) had a spiral cavity of width 4

mm, thickness 2 mm, and maximum flow length 35 mm. The mould cross-section was a semi-circle.

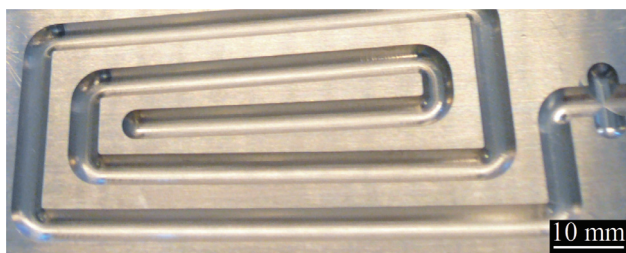


Figure 1. Spiral mould.

Rheological measurements were taken by using a rotational rheometer (Physica MCR 301) with a parallel-plate geometry. Three to seven hot-pressed disc samples were piled up to form specimens with a diameter of 25 mm and a thickness of 0.6 mm. A temperature/frequency sweep method was selected with a frequency range of 1–550 rad/s at 200 °C. The strain rate was taken as 5%. All samples were oven-dried at 80 °C for several hours and then tested under a continuous nitrogen purge to prevent moisture-induced and oxidative degradation of polyamide.

Dynamic mechanical analysis (DMA) was done using a Perkin Elmer Pyris Diamond DMA, operating in single cantilever mode at an oscillation frequency of 1.0 Hz and in a temperature range of -80 to 110°C. Measurements were taken under nitrogen at a 2°C/min heating rate. Specimens with approximate dimensions of 10 x 5 x 2 mm³ were cut from injection-moulded tensile test bars (1BA test bar according to SFS-EN ISO 527-2), and their edges and surfaces were polished with sandpaper. The storage modulus (E'), the loss factor ($\tan \delta$), and the glass transition temperatures (T_g) were determined. T_g was taken from the peak of the $\tan \delta$ curve. The reported (Table 3) E' values at specific temperatures and the glass transition temperatures (T_g) represent the averaged results of approximately three DMA runs.

RESULTS

Raw material characterization

Characterization of 40-nm ALD-coated PA particle was done using a SEM (Figure 1). The cross-section image of a powder particle shows clear contrast variation on its border, implying that the brightest, narrow ribbon-shaped area contains the most titanium whereas the darkest areas, i.e., the polyamide and epoxy matrix (where the PA particle was cast), contains no titanium at all.

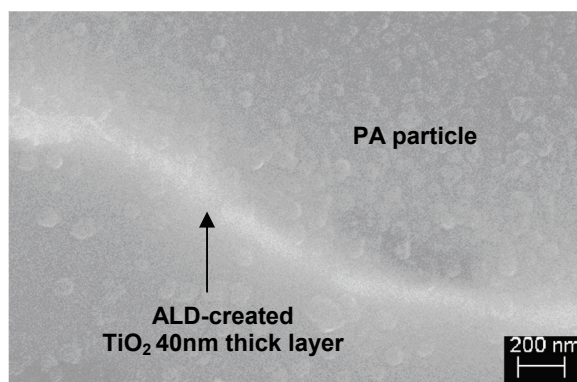


Figure 2. ESB cross-sectional SEM of 40-nm TiO₂ coated PA particle.

Due to the sample preparation method, the TiO₂ ribbon on the surface of the PA particle looks hazy. The SEM image, however, suggests that the TiO₂ film is rather uniform and smooth. Similar results have been obtained^{4,5} on alumina-coated high density polyethylene particles. Specner et al.⁴ and Liang et al.⁵ established a model of the growth mechanism of an alumina layer on a polymer particle, suggesting that during the coating process the pores on the particle surface become smaller and after several coating cycles, alumina clusters form a continuous layer on the polymer particle surface.

A melt mass flow rate (MFR) measurement was taken to approximate the rheological properties of the studied polyamide powders before melt-compounding. MFR results show (Table 1) a melt mass flow rate (MFR) of 3 g/10 min for the unfilled polymer but 7 to 11 times higher values for the ALD-created nanocomposites.

This drastic increase in the MFR, and thus a reduction in viscosity, reported also in our previous paper⁶, contradicts several studies on traditionally filled polyamide nanoclay nanocomposites¹¹⁻¹³. MFR results presented in this paper, therefore, confirm that the viscosity decrease demonstrated at rather high rotational frequencies (0.1–550 rad/s refers also to a high shear rate) in the rotational rheometer is evident at significantly lower shear rates too.

Table 1. Melt-mass flow rates of PA nanocomposite raw materials.

Identification	Content		Melt-mass flow rate (g/10 min)
	PA (wt.%)	ALD-coated (wt.%)	
Reference PA	100	0	3 ± 0.2
100% PA 10 nm	0	100	23 ± 3.0
100% PA 40 nm	0	100	32 ± 0.1

Melt flow properties

A spiral mould tool was used for relative comparison of the final flow length of different nanocomposite polyamides. The polymer flow in the spiral mould stops when solidified layers on upper and lower cavity walls converge, restricting further polymer flow through the cavity¹⁴. A packing phase does not occur because the flow does not reach the end of the spiral mould. Even though spiral flow predictions fail to account for a radial flow inherent in most real parts¹⁵, the spiral flow test is considered a rapid method to estimate the material's ability to fill a part.

Spiral flow results (Figure 3 and Table 2) show that ALD-created nanocomposites possess longer spiral length than pure PA. Their spiral length increases linearly as the ALD-coated polyamide particle content increases in the composite. The increase in the spiral length for a composite containing

25 wt.% of ALD-coated particles was about 15% whereas that for 100 wt.% ALD-coated material was as high as 80% compared to pure polyamide.

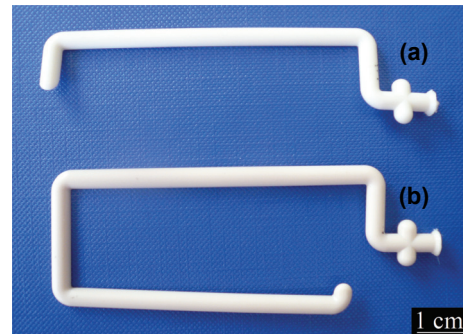


Figure 3. Melt flow spiral length comparison, (a) reference PA of length 10.2 mm and (b) 100% PA 10-nm TiO₂ nanocomposite of length 18.1 mm.

Generally, the capability of a polymer melt to flow in the injection moulding process is a function of temperature and shear-rate-dependent viscosity¹⁴. These parameters were, however, kept constant during the melt flow spiral test. The increase in the MFR may thus be traced to two factors: (1) flow improvement by ALD-created TiO₂ due to polymer chain slipping over TiO₂ fillers and/or (2) due to a molecular weight reduction following the degradation and chain scission of the polyamide matrix during melt-compounding, as suggested by other authors for polyamide nanocomposites^{6,16,17}. Our previous study on ALD-coated nanocomposites suggested no significant thermal degradation, as demonstrated by the similar viscoelastic and thermal behaviour between the ALD-created nanocomposites and pure PA. In the following, experiments on the effect of dilution on complex viscosity and thermal properties are discussed in detail.

Table 2. Melt flow spiral length and complex viscosity results (at frequency of 10 rad/s) of studied polyamide nanocomposites.

Identification	Content		Spiral length (mm)	Complex viscosity at 10 rad/s (Pa·s)
	PA (wt.%)	ALD-coated (wt.%)		
Reference PA	100	0	10.2 ± 0.3	2407 ± 345
25% PA 10 nm	75	25	11.8 ± 0.7	1213 ± 81
50% PA 10 nm	50	50	13.7 ± 1.0	644 ± 40
75% PA 10 nm	25	75	15.7 ± 0.2	380 ± 22
100% PA 10 nm	0	100	18.1 ± 0.7	190 ± 48
100% PA 40 nm	0	100	-	30 ± 66

Complex viscosity results

The complex viscosity results shown (Table 2 and Figure 4a) for the ALD-created polyamide composites and reference PA demonstrate that the viscosity decreased systematically as a function of the ALD-created TiO₂-filler content. Compared to pure PA, the highest reduction in complex viscosity was obtained for the 40-nm ALD-coated polyamide composite. The results imply that by using ALD-coated polymer powder as an additive, the viscosity of the host matrix can be tailored to a desired level, first, by changing the dilution percentage and, second, by changing the thickness of the ALD-coating on a polymer particle. The effect of the ALD-coating thickness must be viewed with care because only two thicknesses were studied. Furthermore, comparing these results to our previous studies⁶, we can see that the present complex viscosity values of the 100% 40-nm, ALD-created composite are somewhat lower than in our previous paper⁶. Such behavior may stem mainly from the different type of specimen. Here several hot-pressed disc samples were piled up to form 0.6-mm thick specimens whereas previously we used coin-shaped injection moulded samples.

By replotting the complex viscosity values at a certain frequency and as a function of the melt flow spiral length (Figure 4b) for ALD-created polyamide composites, we obtain a linear correlation. The linear correlation shown in

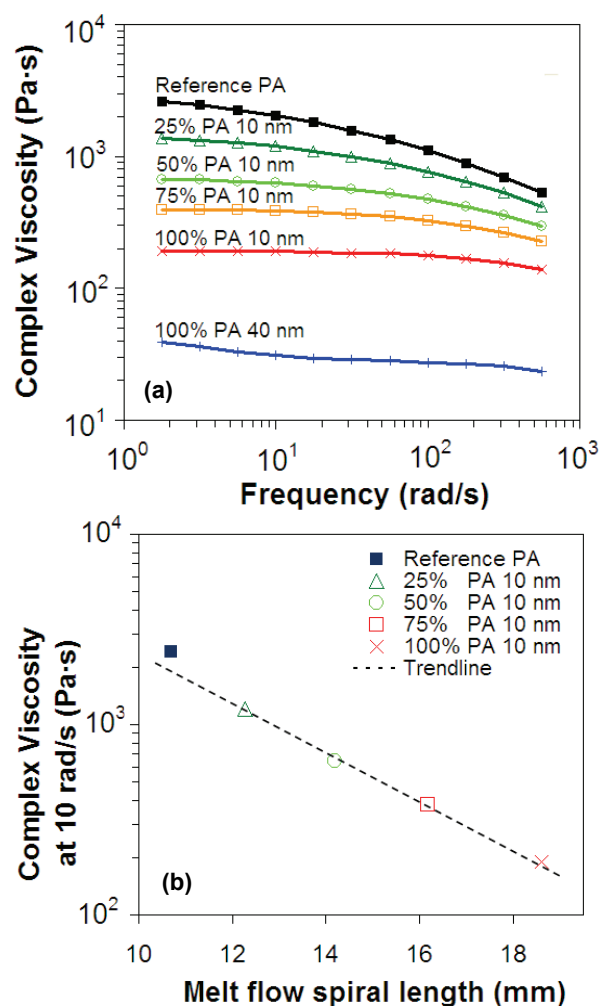


Figure 4. Complex viscosity as a function of (a) frequency and (b) melt flow spiral length for PA TiO₂ nanocomposites at 200°C.

Figure 4b suggests that the ALD-created nanomaterial content in polyamide is a key parameter in terms of viscosity decrease over a broad range of melt flow shear rates. Furthermore, the complex viscosity value at certain shear rate (e.g. 10 rad/s) can be estimated surprisingly accurately using a spiral mould test instead of resorting to time-consuming and expensive rotational rheometer measurements.

Thermal properties

The DMA method used here was taken as a first approximation to examine molecular weight changes in the specimens and further to explain the rheological behaviour of the ALD-created and diluted nanocomposites (Figure 5). It is expected that if changes occur in samples' molecular weight, their viscoelastic behaviour changes too^{18,19} because thermal properties depend, among other things, on molecular weight and the extent of branching and crosslinking in the polymer matrix¹⁸.

Figure 5 shows the storage modulus E' and loss factor $\tan \delta$ as a function of temperature for the prepared samples. According to E' curves at temperatures below the glass transition ($T < 40^\circ\text{C}$) E' , the values of ALD-created composites are higher or identical to pure PA. In general, the average E' values of tree parallel measurements at different temperatures (Table 3) suggest that within the experimental error, the E' value remains unchanged for the studied samples, demonstrating that the viscoelastic behaviour of the prepared nanocomposites and thus the molecular weight of the PA matrix did not significantly change. This is also supported by the loss factor $\tan \delta$ curves, where the nanocomposite peak does not shift compared to pure PA, indicating an unchanging T_g for the studied materials (Table 3).

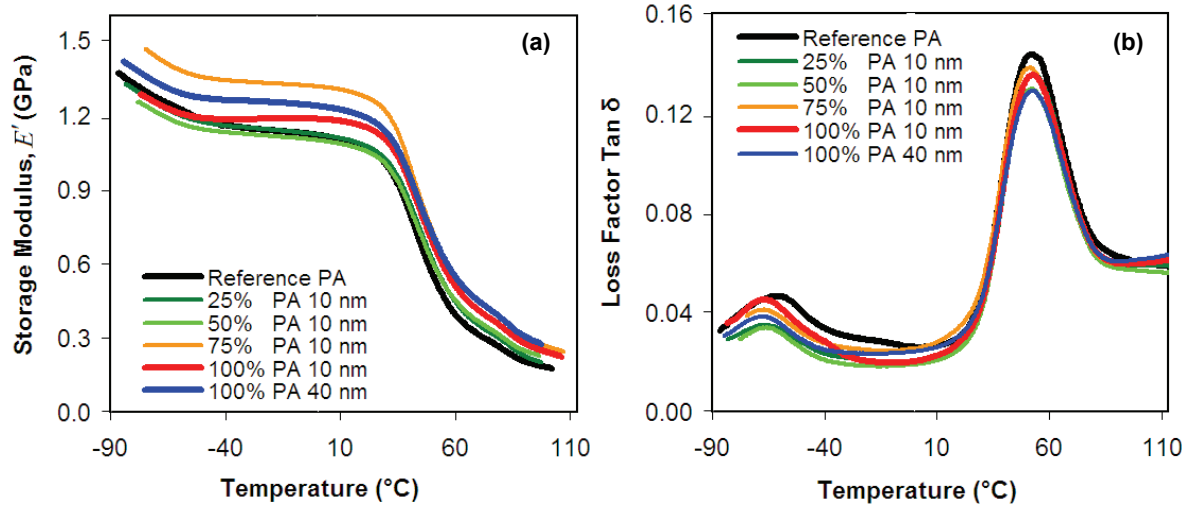


Figure 5. DMA results of (a) storage modulus, E' , and (b) loss factor ($\tan \delta$) as a function of temperature for ALD-created PA / TiO_2 nanocomposites and reference PA.

Table 3. Dynamic mechanical analysis results of studied PA nanocomposites.

Identification	E' at -40 °C ^a (GPa)	E' at +20 °C ^a (GPa)	T _g ^b (°C)
Reference PA	1.2	1.2	52
25% PA 10 nm	1.2	1.1	52
50% PA 10 nm	1.1	1.0	51
75% PA 10 nm	1.3	1.2	51
100% PA 10 nm	1.2	1.1	53
100% PA 40 nm	1.2	1.2	53

^a Determined from E' curves standard deviation value being ± 0.1 .

^b Determined from peak on $\tan \delta$ curve standard deviation value being ± 1 .

DISCUSSION

Clearly, good processing properties, including sufficiently low viscosity, are important in injection moulding to avoid incomplete mould filling. Hence, creating nanocomposites by ALD becomes very attractive, e.g., for micro-injection moulding. However, the origin of the decrease in viscosity, demonstrated by the increase in the melt-mass flow rate and the melt flow spiral length and the decrease in the complex viscosity is not yet fully understood and calls for further study.

In our work, thermal tests clearly suggested that the polyamide matrix did not markedly degrade because viscoelastically the reference polyamide material and ALD-created polyamide nanocomposites behaved similarly. Therefore, viscosity may decrease because of some complex phenomenon during melt-compounding. Apparently, a number of factors may contribute to the viscosity drop we observed. For example, ALD-created TiO₂ filler properties such as surface friction, hardness, and the interaction of two TiO₂-coated particles as well as polymer composite properties such as mechanical properties, thermal conductivity, and moisture content may significantly affect viscosity.

Furthermore, titanium-based ceramic materials like titanate are also known to be employed as coupling agents in filled polymer systems to lower viscosity. For example, Wah et al.²⁰ demonstrated that in

polypropylene talc composites, a titanate coupling agent increased the melt flow index. However, the mechanism of such viscosity decrease is still unknown.

One explanation of the ALD coating effect on decreased viscosity may be the low adhesion and friction properties between the two ceramic surfaces, namely the ALD-coated TiO₂ polyamide particles, before the TiO₂ shells are crushed during melt-compounding. Shell remnants in the polymer matrix are apparently firmly attached to polymer chains originally located on the surface of the polymer powder whereas the surface side of the coating has low friction; consequently, lubricating / plasticizing action occurs in the polyamide system. Thus the ALD-created TiO₂ improves the flow most likely because polymer chains keep slipping over the TiO₂ fillers.

Another factor affecting the viscosity could be the transition from shear flow of unfilled polymer to near-wall slip. The higher the concentration of ALD-created polyamide, the stronger the structural basis of the filler in the polymer melt and the easier the transition to a near-wall slip. In a near-wall slip, the melt flows by slipping along the walls of the moulding system without adhesive sticking. Consequently, the orientation of the polymer molecules and TiO₂ ribbons in the flow direction and the wall-slip undoubtedly play a major role in reducing the viscosity. This is what explains the rheological behaviour of thermoplastics reinforced with carbon fibers²¹. However, we do not yet know exactly the mechanism behind the viscosity decrease in ALD-created polyamide nanocomposites.

CONCLUSIONS

In this work, we demonstrated that ALD-created material has easier melt-processing properties than a pure polyamide matrix because of a significantly lower viscosity. The spiral flow length and the complex viscosity of the diluted specimens behaved linearly as a function of ALD-coated polyamide particle content, suggesting that ALD-coated materials can be applied

additively and cost-effectively to tailor the rheological properties of a polyamide matrix.

Furthermore, similar DMA curves for nanocomposites and pure polyamide demonstrated that the lower viscosity of the ALD-coated polyamide nanocomposites is not only linked to the degradation or chain scission of the polymer during processing. Apparently, flow improvement by ALD-created TiO₂ due to polymer chain slipping over TiO₂ fillers and/or ALD-created TiO₂ adheres poorly to the walls during extrusion and in the moulding system, and acts as a lubricating/plasticizing agent that lowers the viscosity. However, the mechanism of the lowered viscosity is not yet fully understood.

ALD-created polymer nanocomposite material, boasting low melt viscosity and no deterioration of thermal properties, offers great opportunities for developing new products and markets, e.g., in the injection moulding of thin-walled micro-parts. With its low viscosity, this material fills small moulds perfectly without trapping air. However, intensive research is required to examine the effects of ALD coatings on different material combinations.

ACKNOWLEDGMENTS

Financial support from the Finnish Funding Agency for Technology and Innovation and The Graduate School of the Processing of Polymers and Polymer-Based Multimaterials are gratefully acknowledged. We are also grateful to Dr. Janne Sundelin, Mr. Juha-Pekka Pöyry, and Ms. Sinikka Pohjonen for the scanning electron microscope pictures, rotational rheometer information, and dynamic mechanical analysis information, respectively.

REFERENCES

1. Ritala, M. and Leskelä, M. (1999), "Atomic layer epitaxy – a valuable tool for nanotechnology", *Nanotechnology*, **10**, 19-24.
2. Leskelä, M. and Ritala, M. (2002), "Atomic layer deposition (ALD): from

precursors to thin film structures", *Thin Solid Films*, **409**, 138-146.

3. Leskelä, M., Kemell, M., Kukli, K., Pore, V., Santala, E., Ritala, M. and Lu, J. (2007), "Exploitation of atomic layer deposition for nanostructured materials", *Mat. Sci. and Eng., C* **27**, 1504-1508.

4. Spencer, J.A., Liang, X., George, S.M., Buechler, K.J., Blackson, J., Wood, C.J., Dorgan, J.R. and Weimer, A.W. (2007), "Fluidized Bed Polymer Particle ALD Process for Producing HDPE/Alumina Nanocomposites", *ECI Conference on The 12th International Conference on Fluidization - New Horizons in Fluidization Engineering*, Vancouver, Canada, **RP4**, 417-424.

5. Liang, X., Hakim, L.F., Zhan, G.-D., McCormick, J.A., George, S.M., Weimer, A.W., Spencer, J.A., Buechler, K.J., Blackson, J., Wood, C.J. and Dorgan J.R. (2007), "Novel Processing to Produce Polymer/Ceramic Nanocomposites by Atomic Layer Deposition", *J. Am. Ceram. Soc.*, **90**, 57-63.

6. Nevalainen, K., Sundelin, J., Vuorinen, J., Villman, V., Suihkonen, R., Järvelä, P., and Lepistö, T. (2008), "Comparison between Melt Compounded Nanocomposites of Atomic-Layer-Deposition-Coated Polyamide Particles and Traditional Nanofillers", *ECCM-13, 13th European Conference on Composite materials*, June 2-5.2008 Stockholm, Sweden, 10 p.

7. Hecke, M. and Schomburg W.K. (2004), "Review on micro molding of thermoplastic polymers", *J. Micromech. Microeng.* **14**, R1-R14.

8. Greener, G. and Wimberger-Friedl, R. (2006), "Precision Injection Molding: Process, Materials, and Applications", Hanser Gardner Publications, pp. 1-11.

9. King D.M., Spencer, J.A., Liang, X., Hakim, L.F., Weimer, A.W. (2007), "Atomic layer deposition on particles using a fluidized bed reactor with in situ mass spectrometry", *Surface and Coatings Technology*, **201**, p. 9163-9171.
10. EOS GmbH. (2008), "Product Information EOSINT P / PA2200-Pulver", *Manufacturer Supplied Materials Data Sheet*, 12 p.
11. Kim, J.H. and Creasy, T. S., (2004), "Measurement of Sintering Characteristics of Clay-Reinforced Polyamide 6 Nanocomposite", *Polymer Testing*, **23**, 629-636.
12. Chow, W.S., Ishak, Z.A.M., Ishiaku, U.S., Karger-Kocsis, J., and Apostolov, A.A. (2004), "The effect of organoclay on the mechanical properties and morphology of injection-molded polyamide 6/polypropylene nanocomposites", *J. Applied Polym. Sci.*, **91**, 175-189.
13. Chow, W.S., Ishak, Z.A.M., and Karger-Kocsis, J. (2005), "Morphological and Rheological Properties of Polyamide 6/Poly(propylene)/Organoclay Nanocomposites", *Macromol. Mater. Eng.*, **290**, 122-127.
14. Buchmann, M., Theriault, R. and Osswald, T. A. (1997), "Polymer flow length simulation during injection mold filling", *Polym. Eng. Sci.*, **37**, 667-671.
15. Poslinski, A., Fox, C., and Kazmer, D. (1998), "Correlation Of Spiral And Radial Flow Lengths For Injection-Molded Thermoplastics," in *Proceeding of the Society of Plastics Engineers Annual Technical Conference*, 1998. Atlanta, GA. 5 p.
16. McNally, T., Murphy, W. R., Lew, C. Y., Turner, R. J., and Brennan, G.P. (2003), "Polyamide-12 layered silicate nanocomposites by melt blending", *Polymer*, **44**, 2761-2722.
17. Kim, G.-H., Lee, D.-H., Hoffmann, B., Kressler, J., and Stöppelmann, G. (2001), "Influence of nanofillers on the deformation process in layered silicate/polyamide-12 nanocomposites", *Polymer*, **42**, 1095-1100.
18. Ehrenstein G.W, Riedel, G., and Trawiel, P. (2004), "Thermal Analysis of Plastics, Theory and practice", Hanser Publishers, Munich, pp. 236-294.
19. Kim, Y.W., Park, J.T., Koh, J.H., Min B.R., Kim, J.H., (2008), "Molecular thermodynamic model of the glass transition temperature: dependence on molecular weight", *Polymers Adv Tech.*, Published online in Wiley InterScience. 3 p.
20. Wah, C.A., Choong, L.Y., and Neon, G.S. (2000), "Effects of titanate coupling agent on rheological behaviour, dispersion characteristics and mechanical properties of talc filled polypropylene", *Eur. Polym. J.*, **36**, 789-801.
21. Kotomin, S.V, Dreval, V.E., Markov, A.G., and Malchanov, B.I. (1994), "Rheological characteristics of processing of thermoplastics reinforced with carbon fibres", *Fibre Chemistry*, **26**, 357-360.